2-2017

Contribution of Pentose Catabolism to Molecular Hydrogen Formation by Targeted Disruption of Arabinose Isomerase (*araA*) in the Hyperthermophilic Bacterium *Thermotoga maritima*

Derrick White
University of Nebraska - Lincoln, derrick.white@yahoo.com

Raghuveer Singh
University of Nebraska - Lincoln, raghuveer@huskers.unl.edu

Deepak Rudrappa
University of Nebraska–Lincoln, deepakgr@unl.edu

Jackie Mateo
University of Nebraska-Lincoln

Levi Kramer
University of Nebraska-Lincoln, lkramer4@unl.edu

See next page for additional authors

AMERICAN SOCIETY FOR MICROBIOLOGY | Applied and Environmental Microbiology®

GENETICS AND MOLECULAR BIOLOGY

Contribution of Pentose Catabolism to Molecular Hydrogen Formation by Targeted Disruption of Arabinose Isomerase (*araA*) in the Hyperthermophilic Bacterium *Thermotoga maritima*

Derrick White,[a] Raghuveer Singh,[a] Deepak Rudrappa,[a] Jackie Mateo,[a] Levi Kramer,[b] Laura Freese,[a] Paul Blum[a]

School of Biological Sciences[a] and Department of Chemical and Biomolecular Engineering,[b] University of Nebraska—Lincoln, Lincoln, Nebraska, USA

ABSTRACT *Thermotoga maritima* ferments a broad range of sugars to form acetate, carbon dioxide, traces of lactate, and near theoretic yields of molecular hydrogen (H_2). In this organism, the catabolism of pentose sugars such as arabinose depends on the interaction of the pentose phosphate pathway with the Embden-Myerhoff and Entner-Doudoroff pathways. Although the values for H_2 yield have been determined using pentose-supplemented complex medium and predicted by metabolic pathway reconstruction, the actual effect of pathway elimination on hydrogen production has not been reported due to the lack of a genetic method for the creation of targeted mutations. Here, a spontaneous and genetically stable *pyrE* deletion mutant was isolated and used as a recipient to refine transformation methods for its repair by homologous recombination. To verify the occurrence of recombination and to assess the frequency of crossover events flanking the deleted region, a synthetic *pyrE* allele, encoding synonymous nucleotide substitutions, was used. Targeted inactivation of *araA* (encoding arabinose isomerase) in the *pyrE* mutant was accomplished using a divergent, codon-optimized *Thermosipho africanus pyrE* allele fused to the *T. maritima groES* promoter as a genetic marker. Mutants lacking *araA* were unable to catabolize arabinose in a defined medium. The *araA* mutation was then repaired using targeted recombination. Levels of synthesis of H_2 using arabinose-supplemented complex medium by wild-type and *araA* mutant cell lines were compared. The difference between strains provided a direct measurement of H_2 production that was dependent on arabinose consumption. Development of a targeted recombination system for genetic manipulation of *T. maritima* provides a new strategy to explore H_2 formation and life at an extremely high temperature in the bacterial domain.

IMPORTANCE We describe here the development of a genetic system for manipulation of *Thermotoga maritima*. *T. maritima* is a hyperthermophilic anaerobic bacterium that is well known for its efficient synthesis of molecular hydrogen (H_2) from the fermentation of sugars. Despite considerable efforts to advance compatible genetic methods, chromosome manipulation has remained elusive and hindered use of *T. maritima* or its close relatives as model hyperthermophiles. Lack of a genetic method also prevented efforts to manipulate specific metabolic pathways to measure their contributions to H_2 yield. To overcome this barrier, a homologous chromosomal recombination method was developed and used to characterize the contribution of arabinose catabolism to H_2 formation. We report here a stable genetic

Received 15 September 2016 **Accepted** 21 November 2016

Accepted manuscript posted online 9 December 2016

Citation White D, Singh R, Rudrappa D, Mateo J, Kramer L, Freese L, Blum P. 2017. Contribution of pentose catabolism to molecular hydrogen formation by targeted disruption of arabinose isomerase (*araA*) in the hyperthermophilic bacterium *Thermotoga maritima*. Appl Environ Microbiol 83:e02631-16. https://doi.org/10.1128/AEM.02631-16.

Editor Haruyuki Atomi, Kyoto University

Address correspondence to Paul Blum, pblum1@unl.edu.

method for a hyperthermophilic bacterium that will advance studies on the basic and synthetic biology of *Thermotogales*.

KEYWORDS genetic systems, extremophiles, biohydrogen, homologous recombination, anaerobes

Thermotoga maritima is a hyperthermophilic anaerobic bacterium that ferments simple sugars to H_2, acetate, lactate, and carbon dioxide (1). In complex medium (CM) it grows optimally at 80°C with a generation time of 75 min (1). Because of its rapid growth and aerotolerance, it has been the recipient of considerable investigative effort. This included genome sequencing (2–6), comprehensive functional genomics for protein structural characterization (5, 7), and transcriptomic studies using oligonucleotide arrays (8–16). However, in the absence of a genetic system for genome manipulation, its use as a model hyperthermophile has not been realized.

There have been advances in genetic methods for *T. maritima*. Marker selection strategies used the analog 2-deoxyglucose to recover resistant mutants in an effort to use sugar utilization genes as a marker (17). Spheroplast-based transformation was developed that removed the proteinaceous toga to promote DNA uptake using liposomes (18). Finally, plasmids were evaluated that encoded heat-stable antibiotic resistance for selection at elevated growth temperatures (18–21). Despite these approaches, however, manipulation of the chromosome has remained elusive.

The impact of pentose metabolism on H_2 synthesis is crucial for biohydrogenesis applications using a fermentative organism such as *T. maritima*. This is because a significant proportion of lignocellulosic plant feedstocks is made of 5-carbon sugars such as xylose and arabinose. These sugars are metabolized via the pentose phosphate pathway (PPP), which consists of oxidative and nonoxidative components. The main function of the nonoxidative pathway is to generate C_3 through C_7 sugars from ribose 5-phosphate. These can be used for nucleic synthesis and can enter the oxidative pentose phosphate pathway to support production of ATP and reductant. Pentose metabolism has been studied only recently in *Thermotoga* species, where a H_2 yield of 3.33 mol per mol of sugar was reported (22). To better understand the contribution of arabinose to H_2 formation through pentose catabolism, a method for homologous chromosomal recombination was developed and used to inactivate catabolism of this sugar by targeted mutation of *araA*, which is involved in the first step in arabinose catabolism.

RESULTS

Isolation and characterization of *T. maritima pyrE* mutants. The development of a *T. maritima* genetic system required a series of components, including a genetic marker, a marker-compatible medium, a specialized host strain, a suicide vector, an effective transformation method, and a chromosomal recombination event. A genetic marker that conferred pyrimidine prototrophy was developed through the isolation of spontaneous *pyrE* mutants. A defined solid medium was needed for clonal isolation of mutants to determine their genetic stability and to recover recombinants. A defined liquid medium was needed to verify strain phenotypes and, in some cases, to enrich for rare recombinants. Uracil auxotrophs were recovered by the selection of isolates resistant to 5-fluoroorotic acid (5-FOA) (23) using a solid medium. This occurred at a frequency of 10^{-7} at an 5-FOA concentration of 400 μg/ml. DNA sequence analysis of *pyrE* (THMA_RS01695) and *pyrF* (THMA_RS01700) from 10 resistant isolates indicated that all encoded loss-of-function mutations in *pyrE*, whereas *pyrF* remained unaffected. These isolates all encoded the same *pyrE* mutation (*pyrE*-64) that consisted of a 2-nucleotide (nt) deletion (−TG) at chromosomal positions 351792 (−T) and 351793 (−G), 155 nt from the 3′ end of *pyrE* (Fig. 1A). This mutation resulted in a premature stop codon (TGA) 64 nt before the natural stop codon and therefore reduced the length of orotate phosphoribosyl transferase by 21 amino acids (aa) from the original 187 aa. An auxotrophic phenotype for this isolate was not confirmed by growth in a defined

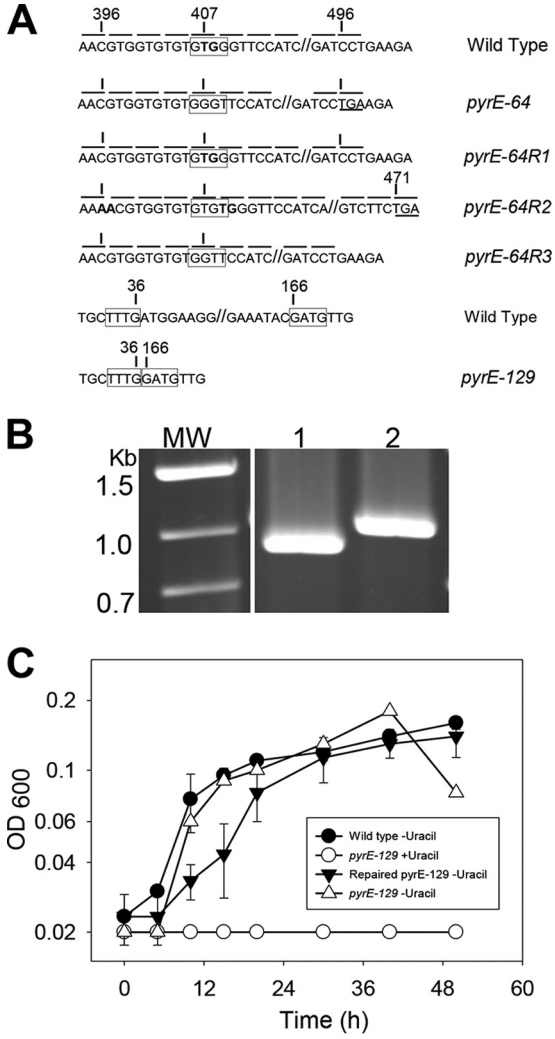

FIG 1 Genotypic analysis, DNA sequence, and growth curve of the *pyrE*-129 mutant. (A) DNA sequence of the *pyrE*-64 mutant, its revertants, and the *pyrE*-129 mutant. The highlighted and boxed nucleotide sequence indicates sites of the deletion and insertion events in mutant strains. The numbers indicate the location of the deletion and insertion within the *pyrE* gene in all five strains. (B) PCR amplification of the *pyrE* allele using genomic DNA from the *pyrE*-129 mutant (lane 1) and the wild type (lane 2). (C) Growth of the *pyrE*-129 mutant, the wild type, and the repaired *pyrE*-129 mutant in a defined medium (DM) with or without uracil supplementation. The image of the gel was modified by cropping intervening lanes.

medium without uracil supplementation. The *pyrE*-64 mutation reverted at a frequency of 10^{-7} as a result of several types of mutations. These included a 2-nt insertion located at chromosomal positions 351792 (T) and 351793 (G) (*pyrE*-64R1) that restored the original reading frame (Fig. 1A). A second reversion mutation consisted of repair of the original 2-nt deletion by reinsertion of the missing bases combined with a second 2-nt insertion located at chromosomal positions 351783 (A) and 351784 (A) (*pyrE*-64R2). This mutation also shifted the reading frame and resulted in a premature stop codon (TGA) 89 nt before the natural stop codon that truncated the protein length by 30 aa (from an original 187 aa). A third reversion mutation consisted of a single-nucleotide deletion at chromosomal position 351791 (G), along with the original 2-nt deletion (*pyrE*-64R3), thereby restoring the natural reading frame (Fig. 1A) and truncating the protein length to 186 aa from an original 187 aa.

While *pyrE*-64 was relatively stable, a nonreverting mutation was pursued to improve the likelihood of recovery of recombinants. In this case, additional 5-FOA-resistant mutants were isolated from 10 independent cultures. PCR amplification of *pyrE* from one of these isolates produced a smaller amplicon consistent with deletion

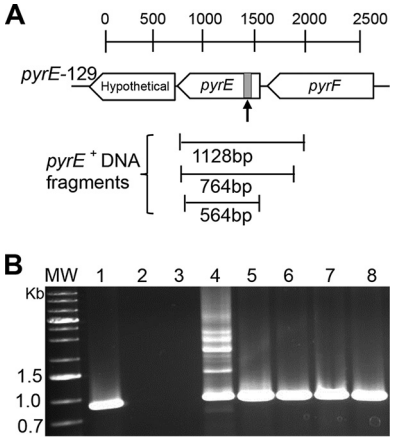

FIG 2 Schematic representation of the *pyrE* locus and wild-type *pyrE* DNAs for repair of the *pyrE*-129 mutant. (A) Genomic environment of the *pyrE*-129 mutation. The gray bar indicates the location of the 129-nt deletion in *pyrE*. The scale bar indicates 500-bp increments across the *pyrE* locus and the various lengths of wild-type DNA fragments used for allele replacement. (B) PCR analysis of *pyrE*$^+$ recombinants with a forward primer complementary to wild-type sequence absent in *pyrE*-129. Lane 1, wild type; lane 2, *pyrE*-129; lane 3, no DNA; lanes 4 to 8, *pyrE*$^+$ recombinants.

formation (Fig. 1B). DNA sequence analysis indicated it encoded a 129-nt deletion of *pyrE* located at the 5′ end of the gene at nt 37 that spanned chromosomal positions 351423 to 351552 (Fig. 1A). This in-frame mutation was called *pyrE*-129, and it reduced protein length by 42 aa. An auxotrophic phenotype was confirmed by demonstrating growth in a defined medium was dependent upon uracil supplementation (Fig. 1C). Reversion analysis demonstrated *pyrE*-129 had improved genetic stability, with a reversion frequency of $<10^{-8}$. It was therefore more suitable for use as a recipient to develop targeted chromosomal recombination.

Homologous chromosomal recombination in *T. maritima*. A second required component for the genetic system was a properly designed recombinogenic DNA molecule. The initial design for this molecule considered both its length and topology. (Fig. 2A). The 1,128-bp molecule encoded 500 bp on both sides of the *pyrE*-129 deletion, whereas the 764-bp allele encoded 137 bp of homology 5′ to the deletion and 498 bp 3′ to the deletion. The 564-bp allele encoded 37 bp of homology 5′ to the deletion and 398 bp 3′ to the deletion. Successful enrichment for prototrophic cells, followed by the formation of prototrophic colonies, was observed only for circular forms of the 1,128- and 764-bp molecules.

Transformation using various lengths of methylated and unmethylated linear *pyrE* DNA did not result in liquid enrichment. These results indicated that these two components could not be distinguished without an autonomously replicating vector. Since such vectors have not been reported for *T. maritima*, transformation and recombination were measured together, arising from change in the allelic state of the *pyrE* genetic marker. An initial transformation procedure used spheroplasts as described previously (18). These cells lack at least portions of the toga (outer membrane and proteinaceous wall) and therefore were permeable to DNA transport. They were evident by their spherical morphology rather than normal elongated rod shape (1). The use of spheroplasts was replaced subsequently during this study by the use of natural transformation as described previously for related *Thermotoga* species (19–21). The relative efficiency of recombination using spheroplasts was $1 \times 10^4/\mu$g of DNA, whereas that for natural transformation was $5 \times 10^6/\mu$g of DNA. In contrast to the longer DNA molecules, the shorter 564-bp molecule failed to produce recombinants using spheroplasts or natural transformation despite repeated attempts that followed identical procedures. This suggested a more extended length of DNA homology was required for recombination. Purified isolates recovered using both transformation methods were tested for prototrophic growth relative to controls, and the *pyrE* locus

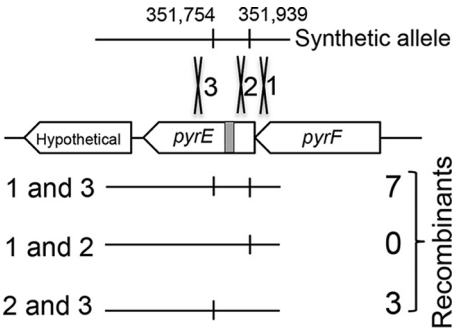

FIG 3 Recombination at the *pyrE* locus. The genomic region of the *pyrE*-129 mutation is indicated by tick marks with coordinates. The gray box indicates the location of the 129-nt deletion. The small black tick lines within the three lines indicate the locations of the synonymous codon changes in the *pyrE* locus of the recombinants. The three X symbols indicate the recombination events resulting in three recombination outcomes when using the synthetic *pyrE* allele.

was examined by PCR and DNA sequencing (Fig. 2B). All subsequent genetic crosses used the natural transformation procedure because of its improved efficiency.

Analysis of recombination using synthetic donor DNA. The occurrence of putative *pyrE* recombinants exhibiting a prototrophic phenotype might arise by contamination from wild-type (WT) cells. To exclude this possibility, a synthetic *pyrE* allele containing two synonymous substitution mutations located at chromosomal positions 531939 and 531754 was used to repair uracil auxotrophy. These substitutions flanked the *pyrE*-129 deletion and were positioned 27 nt from the deletion endpoints. However, initial attempts to recover recombinants using this molecule failed. Because the synthetic DNA was shorter than the previously successful molecules encoding the wild-type *pyrE* allele, longer versions of the synthetic DNA were tested that had extended chromosomal homology. One molecule had the addition of 300 bp 5′ to the *pyrE*-129 deletion but did not produce recombinants. The other molecule included both the 5′ extended region and an additional 530 bp 3′ to the *pyrE*-129 deletion. This symmetrically extended molecule produced recombinants. To assess the relative frequency of crossover events, 10 independent isolates obtained from 10 separate transformation reactions were recovered and analyzed. Of these, seven encoded both synonymous changes, and three encoded only one synonymous change, all located 3′ to the *pyrE*-129 deletion (Fig. 3). Because the addition of the 3′-extended region enabled recovery of recombinants, this region was examined more closely for recombinogenic sequences. A homolog of the *Bacillus subtilis* Chi site consensus sequence, AGCGG, was evident and was located at genome coordinates 351704 and 351977 (upstream of *pyrE*) at the 3′ end of *pyrE*. In *B. subtilis*, during recombination, the Chi sequence is recognized by the ATP-dependent helicase/nuclease AddA. THMA_RS1263 may be an AddA homolog with low identity (22%) to the firmicute sequence; however, an AddB homolog that typically associates with AddA was not apparent in *T. maritima* (24).

Construction and characterization of a *T. maritima* selectable marker. Having demonstrated the occurrence of homologous recombination at the *pyrE* locus, a genetic marker was developed that would allow targeted disruption of other *T. maritima* genes without interference from recombination at the native *pyrE* locus. Two components were required: a divergent allele of *pyrE* lacking homology to the native *T. maritima pyrE* and a strong promoter to drive expression of the divergent *pyrE* allele. The divergent *pyrE* was obtained from *Thermosipho africanus* OB7 (DSMZ 5309) (25). A nucleotide Blast analysis of the *T. africanus pyrE* against *T. maritima pyrE* showed no significant matches, with only 8 nt of contiguous homology. This sequence was selected as preferable to *pyrE* genes from more closely related *Thermotoga* species because of its greater degree of divergence. A synthetic allele of the *T. africanus pyrE* gene was designed by codon optimization to match the codon preference of *T. maritima*. The *T. maritima groES* promoter (P_{groES}) was selected for this purpose because

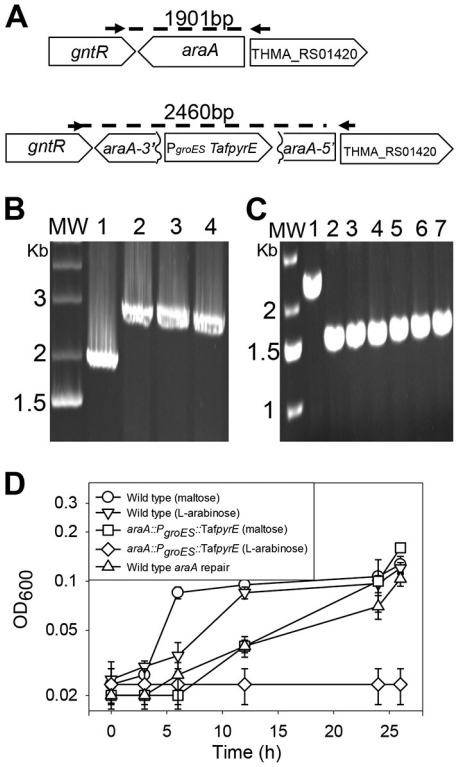

FIG 4 Disruption of *araA*. (A) Schematic representation of homologous recombination at the *araA* locus with the expected size for the *araA* mutant and the wild type using primers within or external to the *araA* locus. The genetic marker was P_{groES}::$pyrE_{Taf}$ (shown as P_{groES} Taf*pyrE* in panel A and P_{groES}::Taf_{pyrE} in panel D). (B) PCR amplification of the disrupted *araA* allele. Lane MW, molecular weight standards; lane 1, wild-type *araA* locus; lanes 2 to 4, *araA* mutant locus. (C) PCR amplification of the repaired *araA* allele. Lane MW, molecular weight standards; lane 1, *araA* mutant; lane 2, wild type; lanes 3 to 7, repaired mutant *araA* loci. (D) Growth curve of the *araA* mutant, wild-type, and *araA* WT repair strains in defined medium with maltose or arabinose. Maltose was used as a positive control for growth.

it had been shown previously to be expressed constitutively during growth of the organism at 80°C (14). The *groES* promoter was 196 nt in length and fused to the *T. africanus* codon-optimized *pyrE*. The resulting divergent genetic marker was called P_{groES} $pyrE_{Taf}$.

Targeted disruption of *T. maritima* chromosomal genes. Inactivation of *araA* (THMA_001415) was then pursued using P_{groES} $pyrE_{Taf}$. Natural transformation of the *pyrE*-129 mutant was performed using the disruption plasmid, pBN1322, containing 5′ and 3′ regions of *araA*, flanking the genetic marker and positioned in a divergent direction relative to the marker (Fig. 4A). Uracil prototrophs were recovered by liquid enrichments, followed by clonal isolation on selective medium plates. PCR analysis using genomic DNA from three isolates, with primers that were complementary to sequences external to the *araA* segments present in plasmid pBN1322, produced amplicons for all isolates that were larger than the wild-type *araA* allele and consistent with the insertion of the genetic marker (Fig. 4B). This prediction was confirmed by DNA sequence analysis that verified the presence of a 763-bp insertion of the P_{groES} $pyrE_{Taf}$ genetic marker at genome coordinate 290557 within *araA*. Phenotypic analysis demonstrated the putative *araA* disruption mutants had lost the ability to catabolize L-arabinose but not maltose relative to the parental strain supplemented with uracil or the unsupplemented wild-type strain (Fig. 4D). One of these isolates, PBL3022, was examined further. To confirm that the mutant phenotype arose specifically as a result of mutation of *araA*, genetic repair of the mutation was necessary. Since an autonomously replicating plasmid-based complementation system for *T. maritima* was not available, repair of the disrupted *araA* allele was conducted using targeted recombi-

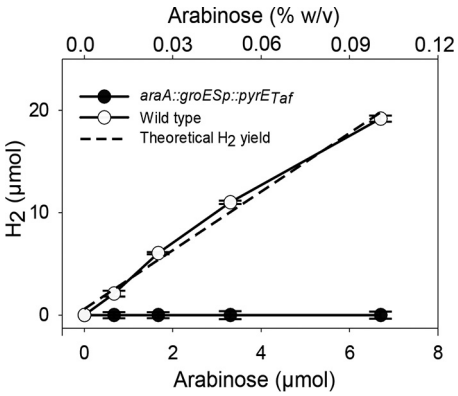

FIG 5 Analysis of H_2 production in the *araA* mutant. H_2 production by the *araA* mutant and parental strain cultivated with various amounts of arabinose was measured. The solid straight line with the closed circles indicates H_2 production by the *araA* mutant. The solid line with the open circle indicates H_2 production by the wild type. The H_2 values are shown as the means of the results from three replicates, with the error bars representing the standard deviations. The dashed line without symbols indicates the theoretical H_2 yield for growth on pentose sugar.

nation. *araA* DNA spanning coordinates 289793 to 291283 was cloned in pBN1323, which was introduced into the *araA* mutant using natural transformation, and enrichment for arabinose utilization was imposed. In addition, FOA was used to inhibit the growth of Pyr^+ cells encoding the P_{groES} $pyrE_{Taf}$ transgene (26, 27). After transformation, the arabinose enrichment culture was plated onto CM plates supplemented with arabinose and 5-FOA, and five isolates were recovered and used for genotypic analysis by PCR. The resulting strains contained the repaired wild-type *araA* allele compared to the *araA* mutant and wild-type controls, as indicated by PCR (Fig. 4C). In addition, the PCR amplicons for three of the five isolates were sequenced and found to be identical to the parental *araA* allele. These same three isolates also regained the ability to catabolize arabinose in liquid culture using a defined medium. Disruption and repair (knock-in and knockout) of *araA* demonstrate the feasibility of targeted chromosomal recombination in *T. maritima*.

Contribution of arabinose catabolism to H_2 formation. Pentose catabolism offers an important route for fermentative H_2 formation since those sugars can be derived from lignocellulosic plant biomass. Although such yields have been predicted using thermodynamic considerations (28) and experimentally by cultivation of wild-type *Thermotoga* species on pentose sugars (8, 10, 22), it has not been shown whether the pentose phosphate pathway (PPP) was the primary route for this process. To measure directly the importance of the PPP for H_2 formation by fermentation of arabinose, it was necessary to use cell lines in which this metabolic pathway had been inactivated, such as through inactivation of *araA*, the gene responsible for the first committed step in the PPP for catabolism of this sugar. Yields of H_2 were determined for the *araA* mutant and its Ara^+ parent cultivated in a complex medium containing added amounts of L-arabinose. Complex medium was used to support cell growth at a moderate level and to ensure that a lack of H_2 production did arise from metabolic inactivity. In addition, a correction for H_2 production arising from fermentation of conventional complex medium additives (yeast extract and tryptone) was made, and this showed that the correct ratio of H_2 per mole of arabinose was 2.97. H_2-mediated growth inhibition (1) was avoided by increasing the culture headspace relative to the culture volume based on experimental reconstructions (22). At L-arabinose concentrations ranging up to 0.1% (wt/vol), the $AraA^+$ parental strain produced H_2 relative to added sugar at a molar ratio of 3.3, whereas no detectable H_2 was produced by the *araA* mutant (Fig. 5). The differences observed in H_2 production between the *araA* mutant and its $AraA^+$ parent across these concentrations of added sugar verify *in vivo* that isomerization of L-arabinose to L-ribulose catalyzed by L-arabinose isomerase is the primary route of

arabinose catabolism leading to H_2 formation. The apparent ratio of H_2 formed to sugar added was consistent with values predicted by the combination of the oxidative and nonoxidative pentose phosphate pathways (22, 29).

DISCUSSION

The establishment of a chromosome engineering method for *Thermotoga maritima* realizes the promise of extensive investments in structural biology and genomics of this organism (2–5, 7, 30). This is important because *T. maritima* may contribute to efforts to create renewable biohydrogen synthesis due to its rapid growth at high temperature. We report here a stable genetic method for a hyperthermophilic bacterium that will advance studies on the basic and synthetic biology of *Thermotogales*. Here, a suite of essential methods, including several predicated on prior studies (18–21), were combined to generate an allele replacement by targeted homologous recombination in *Thermotoga*. In addition to the repair of deleted and disrupted genes and the insertion of synthetic alleles, the specific role of a metabolic pathway toward H_2 synthesis was established.

Pentoses, including xylose and arabinose, are major constituents of lignocellulosic material. Evaluation of arabinose catabolism using a genetic approach demonstrates the importance of the nonoxidative pentose phosphate pathway and its susceptibility for manipulation to perturb H_2 formation. Metabolism of pentoses by *T. maritima* and *T. neapolitana* resulting in H_2 values close to theoretical yields have been reported (22, 29, 31). Here, using a genetic approach, it could be shown directly that arabinose catabolism contributes to H_2 production. H_2 produced in the presence of added sugar was normalized to background levels produced in the absence of added sugar.

This study demonstrates that homologous recombination can be used to modify the *T. maritima* genome. It is therefore interesting to reflect on the native hybrid recombination system in this organism. In particular, *T. maritima* encodes an archaeal/eukaryal Mre11 nuclease instead of the bacterial RecBCD enzymes. Moreover, while *T. maritima* does not encode a eukaryote-like RAD50 homolog, it does encode homologs of eukaryotic RadA (THMA_RS01030) and RadB (TMMA_RS01890) (2). It has been shown that MRE11 can be associated with RAD50 to actively bind DNA. This complex forms a catalytic head that contains an ATP-stimulated nuclease and DNA binding activity that indicates its potential role in processing DNA double-stranded breaks in *T. maritima* (2, 30, 32, 33). It was also found here that a minimum of 100 nt was required for recombination and that a putative recombinogenic sequence (AGCGG) located at the 3′ end of *pyrE* and upstream region of *pyrE* may play a role in recombination at that locus. This sequence may constitute a native Chi-like sequence. In addition, since mutations in both *pyrE* and *araA* were repaired precisely, the presence in *T. maritima* of hybrid eukaryotic-bacterial recombination components does not shift the apparent preference for homologous recombination. Finally, recovery of the synthetic *pyrE* allele encoding synonymous codon changes offers more flexibility in future efforts for engineering the *T. maritima* genome and perhaps an experimental strategy for exploring the biochemistry of this unusual hybrid recombination system.

Additional essential features of the *T. maritima* genetic system include the natural transformation of a genetic marker and a constitutive promoter for genetic marker expression. To further simplify the recombination method, concerted efforts established the existence of natural transformation in *T. maritima*, in contrast to a previous report (20). Since natural transformation was evident, it is worth noting the presence in *T. maritima* of genes likely to encode competence functions, including homologs of the *B. subtilis comEA* and *comFC H. influenzae* DNA processing (*dprA*) and type IV secretion system (*pilA*). The *pyrE* gene was obtained from *T. africanus* because this species is also hyperthermophilic, thus ensuring that the encoded protein would be thermostable, and to reduce sequence identity and thereby avoid unwanted recombination between respective *pyrE* sequences (25). Current applications of the *T. maritima* genetic system concern both metabolic and nonmetabolic targets. They benefit from extensive com-

TABLE 1 *Thermotoga maritima* strains and plasmids

Strain or plasmid	Description	Source
Strains		
PBL3001	*Thermotoga maritima* MSB8	ATCC 45389 (1)
PBL3002	*pyrE*-64	PBL3001
PBL3003	*pyrE*-64R1	PBL3002
PBL3004	*pyrE*-129	PBL3001
PBL3005	*pyrE*-64R2	PBL3002
PBL3006	*pyrE*-64R3	PBL3002
PBL3020	$pyrE^+$ recombinant	PBL3004
PBL3021	$pyrE^+$ recombinant (synthetic *pyrE*)	PBL3004
PBL3022	*araA* 3′::P_{groES} $pyrE_{Taf}$::*araA* 5′ mutant	PBL3004
PBL3028	$araA^+$ recombinant	PBL3022
Plasmids		
pBN1167	pUC19; WT $pyrE^+$ (564 bp)	This study
pBN1183	pUC19; WT $pyrE^+$ (1,120 bp)	This study
pBN1290	pUC19; synthetic $pyrE^+$ (977 bp)	This study
pBN1293	pUC19; WT $pyrE^+$ (764 bp)	This study
pBN1322	pUC19; *araA* 3′:: P_{groES} $pyrE_{Taf}$::*araA* 5′	This study
pBN1333	pUC57; WT $araA^+$ (1,491 bp)	This study

prehensive prior studies about the biology, molecular biology, biochemistry, and metabolism of this bacterial extremophile.

MATERIALS AND METHODS

Strains and cultivation. Unless otherwise indicated, *T. maritima* MSB8 (ATCC 45389, GenBank accession number NZ_CP011107) was cultivated at 80°C under anaerobic conditions (4, 34). Strains of *T. maritima* are listed in Table 1. A complex medium (CM) was prepared as described previously (34). A solid medium was prepared using 6 g of gellan gum (Sigma-Aldrich)/liter. A defined medium (DM), prepared as described previously (34), lacked complex medium additives and contained Wolfe vitamins (35), and the pH was adjusted to 7.0. For the cultivation of uracil auxotrophs; 50 μg of uracil/ml was added to the DM medium as described previously (34). Uracil auxotrophs were isolated as described previously (23) with modifications. Spontaneous 5-FOA-resistant mutants were obtained from independent cultures using CM plates containing 5-FOA (0.4 mg/ml) and uracil (50 μg/ml). Uracil auxotrophy was evaluated by cultivating 5-FOA-resistant mutants in DM with or without uracil supplementation. All growth curves were conducted three times using biological replicates.

***T. maritima* transformation.** The final components for the genetic system were DNA transformation and chromosomal recombination. Two types of transformation methods were used in this study. Artificial transformation used electroporation and spheroplasts. For the preparation of spheroplasts, 50-ml cultures were processed as described previously (18), with the following modifications. DOTAP liposomal reagent (Roche, USA) was removed, a final concentration of 10 mg of proteinase K (MP Biomedicals, USA) was added to the spheroplast mixture, and 50 μl of spheroplast mixture was used for transformation. One microgram of plasmid DNA was added to 50 μl of spheroplast mixture (10^8 cells/ml), electroporated as described previously (19), inoculated into 10 ml of CM, and allowed to recover for 18 to 24 h. Cells were collected by centrifugation and transferred to selective medium. Cultures were incubated at 80°C for 2 to 3 days and then transferred to a selective solid medium to recover clonal isolates. For the preparation of cells for natural transformation, the cells were processed as described previously (20), with modifications. A mixture of exponentially growing cells and plasmid DNA was added to 10 ml of CM, followed by incubation at 80°C for 18 h. The cells were collected by centrifugation, resuspended in 1 ml of DM, and adjusted to a cell density of 10^9 cells/ml by dilution. The cells (10^8/ml) were then inoculated into selective medium for enrichment and plated on defined medium plates to recover recombinants. For the recovery of *araA* WT recombinants, transformed cells were plated onto complex medium plates supplemented with arabinose and 5-FOA, as described previously (26, 27).

Plasmid and strain construction. Repair of the *pyrE*-129 mutant (PBL3004) was performed using native and synthetic alleles of *pyrE*. The native allele varied in length and included fragments 1,120, 764, and 564 bp in length. In addition, a 977-bp synthetic codon-optimized *T. maritima pyrE* allele contained two synonymous codon changes flanking the *pyrE*-129 deletion. All native *pyrE* DNA fragments were cloned into pUC19 at SphI and/or PstI restriction sites and verified by sequencing. Linear DNAs and their circular forms encompassed the *pyrE* open reading frame and included 1,128 bp spanning coordinates 351285 to 352413, 764 bp spanning coordinates 351286 to 352049, and 564 bp spanning coordinates 351386 to 351949. A divergent *pyrE* allele for use as a genetic marker was designed using the *Thermosipho africanus pyrE* gene that was codon optimized for *T. maritima* and fused transcriptionally to the *T. maritima groES* promoter, resulting in the P_{groES} $pyrE_{Taf}$ construct. The promoter-fused *T. africanus pyrE* allele was cloned into the BamHI site of pUC19 (a list of plasmids is provided in Table 1). This insert was flanked by *araA* coding sequences. A 5′ *araA* fragment (746-bp sequence) was cloned at the pUC19 EcoRI/KpnI restriction site, and a 3′ *araA* fragment (745-bp sequence) was cloned at the pUC19 SalI/SphI

restriction site, resulting in plasmid pBN1322 (Table 1). The *araA* disruption mutant (PBL3022) was constructed by integration of the *groESp*::$pyrE_{Taf}$ construct flanked by *araA* sequences at the chromosomal *araA* locus, using the *pyrE*-129 mutant as the recipient, combined with selection for uracil prototrophy. Genomic DNA obtained from independent isolates cultivated in CM without selecting for uracil prototrophy was used to screen for the disrupted *araA* allele by PCR. To repair the *araA* disruption, the full-length wild-type *araA* allele was amplified by PCR and cloned at the EcoRI/SphI restriction site in pUC57.

Hydrogen production. Molecular hydrogen (H_2) was analyzed using a Gow-Mac 400 series gas chromatograph equipped with a molecular sieve column (Gow-Mac, USA). Standard curves were prepared by injecting known amounts of H_2 with a bridge current of 90 mA. The temperatures used for the column, injector, and detector were 70, 90, and 90°C, respectively. Nitrogen (N_2) was used as the carrier gas at a flow rate of 30 ml/min. The H_2 in culture headspace was analyzed in triplicate, and the errors are indicated. The molar yield of H_2 was calculated using the ideal gas law equation ($PV = nRT$) at the standard temperature and pressure. Growth variation among different cell lines in small batch cultures led to H_2 values being normalized to 10^8 cells/ml.

ACKNOWLEDGMENTS

Funding for this study was provided by the Department of Energy and the UNL Cell Development Facility.

REFERENCES

1. Huber R, Langworthy TA, Konig H, Thomm M, Woese CR, Sleytr UB, Stetter KO. 1986. *Thermotoga maritima* sp. nov. represents a new genus of unique extremely thermophilic eubacteria growing up to 90°C. Arch Microbiol 144:324–333.
2. Nelson KE, Clayton RA, Gill SR, Gwinn ML, Dodson RJ, Haft DH, Hickey EK, Peterson JD, Nelson WC, Ketchum KA, McDonald L, Utterback TR, Malek JA, Linher KD, Garrett MM, Stewart AM, Cotton MD, Pratt MS, Phillips CA, Richardson D, Heidelberg J, Sutton GG, Fleischmann RD, Eisen JA, White O, Salzberg SL, Smith HO, Venter JC, Fraser CM. 1999. Evidence for lateral gene transfer between Archaea and Bacteria from genome sequence of *Thermotoga maritima*. Nature 399:323–329. https://doi.org/10.1038/20601.
3. Latif H, Lerman JA, Portnoy VA, Tarasova Y, Nagarajan H, Schrimpe-Rutledge AC, Smith RD, Adkins JN, Lee D-H, Qiu Y, Zengler K. 2013. The genome organization of *Thermotoga maritima* reflects its lifestyle. PLoS Genet 9:e1003485. https://doi.org/10.1371/journal.pgen.1003485.
4. Singh R, Gradnigo J, White D, Lipzen A, Martin J, Schackwitz W, Moriyama E, Blum P. 2015. Complete genome sequence of an evolved *Thermotoga maritima* isolate. Genome Announc 3:e00557-15. https://doi.org/10.1128/genomeA.00557-15.
5. Zhaxybayeva O, Swithers KS, Lapierre P, Fournier GP, Bickhart DM, DeBoy RT, Nelson KE, Nesbø CL, Doolittle WF, Gogarten JP, Noll KM. 2009. On the chimeric nature, thermophilic origin, and phylogenetic placement of the *Thermotogales*. Proc Natl Acad Sci U S A 106:5865–5870. https://doi.org/10.1073/pnas.0901260106.
6. Blum P, Rudrappa D, Singh R, McCarthy S, Pavlik B. 2016. Experimental microbial evolution of extremophiles, p 619–636. *In* Rampelotto HP (ed), Biotechnology of extremophiles: advances and challenges. Springer International Publishing, New York, NY. https://doi.org/10.1007/978-3-319-13521-2_22.
7. Lesley SA, Kuhn P, Godzik A, Deacon AM, Mathews I, Kreusch A, Spraggon G, Klock HE, McMullan D, Shin T, Vincent J, Robb A, Brinen LS, Miller MD, McPhillips TM, Miller MA, Scheibe D, Canaves JM, Guda C, Jaroszewski L, Selby TL, ElsligerM-A, Wooley J, Taylor SS, Hodgson KO, Wilson IA, Schultz PG, Stevens RC. 2002. Structural genomics of the *Thermotoga maritima* proteome implemented in a high-throughput structure determination pipeline. Proc Natl Acad Sci U S A 99:11664–11669. https://doi.org/10.1073/pnas.142413399.
8. Chhabra SR, Shockley KR, Conners SB, Scott KL, Wolfinger RD, Kelly RM. 2003. Carbohydrate-induced differential gene expression patterns in the hyperthermophilic bacterium *Thermotoga maritima*. J Biol Chem 278:7540–7552. https://doi.org/10.1074/jbc.M211748200.
9. Conners SB, Montero CI, Comfort DA, Shockley KR, Johnson MR, Chhabra SR, Kelly RM. 2005. An expression-driven approach to the prediction of carbohydrate transport and utilization regulons in the hyperthermophilic bacterium *Thermotoga maritima*. J Bacteriol 187:7267–7282. https://doi.org/10.1128/JB.187.21.7267-7282.2005.
10. Conners SB, Mongodin EF, Johnson MR, Montero CI, Nelson KE, Kelly RM. 2006. Microbial biochemistry, physiology, and biotechnology of hyperthermophilic *Thermotoga* species. FEMS Microbiol Rev 30:872–905. https://doi.org/10.1111/j.1574-6976.2006.00039.x.
11. Johnson MR, Montero CI, Conners SB, Shockley KR, Bridger SL, Kelly RM. 2005. Population density-dependent regulation of exopolysaccharide formation in the hyperthermophilic bacterium *Thermotoga maritima*. Mol Microbiol 55:664–674.
12. Montero CI, Lewis DL, Johnson MR, Conners SB, Nance EA, Nichols JD, Kelly RM. 2006. Colocation of genes encoding a tRNA-mRNA hybrid and a putative signaling peptide on complementary strands in the genome of the hyperthermophilic bacterium *Thermotoga maritima*. J Bacteriol 188:6802–6807. https://doi.org/10.1128/JB.00470-06.
13. Nanavati DM, Thirangoon K, Noll KM. 2006. Several archaeal homologs of putative oligopeptide-binding proteins encoded by *Thermotoga maritima* bind sugars. Appl Environ Microbiol 72:1336–1345. https://doi.org/10.1128/AEM.72.2.1336-1345.2006.
14. Pysz MA, Ward DE, Shockley KR, Montero CI, Conners SB, Johnson MR, Kelly RM. 2004. Transcriptional analysis of dynamic heat-shock response by the hyperthermophilic bacterium *Thermotoga maritima*. Extremophiles 8:209–217. https://doi.org/10.1007/s00792-004-0379-2.
15. Shockley KR, Scott KL, Pysz MA, Conners SB, Johnson MR, Montero CI, Wolfinger RD, Kelly RM. 2005. Genome-wide transcriptional variation within and between steady states for continuous growth of the hyperthermophile *Thermotoga Maritima*. Appl Environ Microbiol 71:5572–5576. https://doi.org/10.1128/AEM.71.9.5572-5576.2005.
16. Johnson MR, Conners SB, Montero CI, Chou CJ, Shockley KR, Kelly RM. 2006. The *Thermotoga maritima* phenotype is impacted by syntrophic interaction with *Methanococcus jannaschii* in hyperthermophilic coculture. Appl Environ Microbiol 72:811–818. https://doi.org/10.1128/AEM.72.1.811-818.2006.
17. Galperin MY, Noll KM, Romano AH. 1996. The glucose transport system of the hyperthermophilic anaerobic bacterium *Thermotoga neapolitana*. Appl Environ Microbiol 62:2915–2918.
18. Yu JS, Vargas M, Mityas C, Noll KM. 2001. Liposome-mediated DNA uptake and transient expression in *Thermotoga*. Extremophiles 5:53–60. https://doi.org/10.1007/s007920000173.
19. Han D, Norris SM, Xu Z. 2012. Construction and transformation of a *Thermotoga-E. coli* shuttle vector. BMC Biotechnol 12:1–9. https://doi.org/10.1186/1472-6750-12-1.
20. Han D, Xu H, Puranik R, Xu Z. 2014. Natural transformation of *Thermotoga* sp. strain RQ7. BMC Biotechnol 14:1–10. https://doi.org/10.1186/1472-6750-14-1.
21. Xu H, Han D, Xu Z. 2015. Expression of heterologous cellulases in *Thermotoga* sp. strain RQ2. Biomed Res Int 2015:293570. https://doi.org/10.1155/2015/293570.
22. Eriksen NT, Riis ML, Holm NK, Iversen N. 2011. H2 synthesis from pentoses and biomass in *Thermotoga* spp. Biotechnol Lett 33:293–300. https://doi.org/10.1007/s10529-010-0439-x.
23. Vargas M, Noll KM. 1994. Isolation of auxotrophic and antimetabolite-resistant mutants of the hyperthermophilic bacterium *Thermotoga nea-*

politana. Arch Microbiol 162:357–361. https://doi.org/10.1007/BF00263784.
24. Chédin F, Ehrlich SD, Kowalczykowski SC. 2000. The *Bacillus subtilis* AddAB helicase/nuclease is regulated by its cognate Chi sequence *in vitro*. J Mol Biol 298:7–20. https://doi.org/10.1006/jmbi.2000.3556.
25. Huber R, Woese CR, Langworthy TA, Fricke H, Stetter KO. 1989. *Thermosipho africanus* gen. nov., represents a new genus of thermophilic eubacteria within the "*Thermotogales*." Syst Appl Microbiol 12:32–37.
26. Cha M, Chung D, Elkins JG, Guss AM, Westpheling J. 2013. Metabolic engineering of *Caldicellulosiruptor bescii* yields increased hydrogen production from lignocellulosic biomass. Biotechnol Biofuels 6:1–8. https://doi.org/10.1186/1754-6834-6-1.
27. Lipscomb GL, Conway JM, Blumer-Schuette SE, Kelly RM, Adams MWW. 2016. A highly thermostable kanamycin resistance marker expands the tool kit for genetic manipulation of *Caldicellulosiruptor bescii*. Appl Environ Microbiol 82:4421–4428. https://doi.org/10.1128/AEM.00570-16.
28. Reungsang A, Saripan AF. 2013. Biohydrogen production by *Thermoanaerobacterium thermosaccharolyticum* KKU-ED1: culture conditions optimization using mixed xylose/arabinose as substrate. Electron J Biotechnol 16:1–17.
29. Ngo TA, Nguyen TH, Bui HTV. 2012. Thermophilic fermentative hydrogen production from xylose by *Thermotoga neapolitana* DSM 4359. Renewable Energy 37:174–179. https://doi.org/10.1016/j.renene.2011.06.015.
30. Das D, Moiani D, Axelrod HL, Miller MD, McMullan D, Jin KK, Abdubek P, Astakhova T, Burra P, Carlton D, Chiu H-J, Clayton T, Deller MC, Duan L, Ernst D, Feuerhelm J, Grant JC, Grzechnik A, Grzechnik SK, Han GW, Jaroszewski L, Klock HE, Knuth MW, Kozbial P, Krishna SS, Kumar A, Marciano D, Morse AT, Nigoghossian E, Okach L, Paulsen J, Reyes R, Rife CL, Sefcovic N, Tien HJ, Trame CB, van den Bedem H, Weekes D, Xu Q, Hodgson KO, Wooley J, Elsliger M-A, Deacon AM, Godzik A, Lesley SA, Tainer JA, Wilson IA. 2010. Crystal structure of the first eubacterial Mre11 nuclease reveals novel features that may discriminate substrates during DNA repair. J Mol Biol 397:647–663. https://doi.org/10.1016/j.jmb.2010.01.049.
31. de Vrije T, Bakker RR, Budde MA, Lai MH, Mars AE, Claassen PA. 2009. Efficient hydrogen production from the lignocellulosic energy crop *Miscanthus* by the extreme thermophilic bacteria *Caldicellulosiruptor saccharolyticus* and *Thermotoga neapolitana*. Biotechnol Biofuels 2:1–15. https://doi.org/10.1186/1754-6834-2-1.
32. Lammens K, Bemeleit Derk J, Möckel C, Clausing E, Schele A, Hartung S, Schiller-Christian B, Lucas M, Angermüller C, Söding J, Strässer K, Hopfner K-P. 2011. The Mre11:Rad50 structure shows an ATP-dependent molecular clamp in DNA double-strand break repair. Cell 145:54–66. https://doi.org/10.1016/j.cell.2011.02.038.
33. Frock AD, Notey JS, Kelly RM. 2010. The genus *Thermotoga*: recent developments. Environ Technol 31:1169–1181. https://doi.org/10.1080/09593330.2010.484076.
34. Chhabra SR, Shockley KR, Ward DE, Kelly RM. 2002. Regulation of endo-acting glycosyl hydrolases in the hyperthermophilic bacterium *Thermotoga maritima* grown on glucan- and mannan-based polysaccharides. Appl Environ Microbiol 68:545–554. https://doi.org/10.1128/AEM.68.2.545-554.2002.
35. Rinker KD, Kelly RM. 1996. Growth physiology of the hyperthermophilic archaeon *Thermococcus litoralis*: development of a sulfur-free defined medium, characterization of an exopolysaccharide, and evidence of biofilm formation. Appl Environ Microbiol 62:4478–4485.